

## A Palette of Fluorescent Probes with Varying Emission Colors for Imaging Hydrogen Peroxide Signaling in Living Cells

Bryan C. Dickinson,<sup>†</sup> Calvin Huynh,<sup>†</sup> and Christopher J. Chang<sup>\*,†,‡</sup>

Department of Chemistry, Howard Hughes Medical Institute, University of California, Berkeley, California 94720

Received February 17, 2010; E-mail: chrischang@berkeley.edu

**Abstract:** We present a new family of fluorescent probes with varying emission colors for selectively imaging hydrogen peroxide (H<sub>2</sub>O<sub>2</sub>) generated at physiological cell signaling levels. This structurally homologous series of fluorescein- and rhodol-based reporters relies on a chemospecific boronate-to-phenol switch to respond to H<sub>2</sub>O<sub>2</sub> over a panel of biologically relevant reactive oxygen species (ROS) with tunable excitation and emission maxima and sensitivity to endogenously produced H<sub>2</sub>O<sub>2</sub> signals, as shown by studies in RAW264.7 macrophages during the phagocytic respiratory burst and A431 cells in response to EGF stimulation. We further demonstrate the utility of these reagents in multicolor imaging experiments by using one of the new H<sub>2</sub>O<sub>2</sub>-specific probes, Peroxy Orange 1 (PO1), in conjunction with the green-fluorescent highly reactive oxygen species (hROS) probe, APF. This dual-probe approach allows for selective discrimination between changes in H<sub>2</sub>O<sub>2</sub> and hypochlorous acid (HOCl) levels in live RAW264.7 macrophages. Moreover, when macrophages labeled with both PO1 and APF were stimulated to induce an immune response, we discovered three distinct types of phagosomes: those that generated mainly hROS, those that produced mainly H<sub>2</sub>O<sub>2</sub>, and those that possessed both types of ROS. The ability to monitor multiple ROS fluxes simultaneously using a palette of different colored fluorescent probes opens new opportunities to disentangle the complex contributions of oxidation biology to living systems by molecular imaging.

### Introduction

The production of reactive oxygen species (ROS) molecules by biological systems is an inevitable consequence of aerobic life.<sup>1,2</sup> The mismanagement and accumulation of ROS in mammals leads to a condition broadly referred to as oxidative stress, in which the production and destruction of the various cellular oxidants no longer maintains a healthy equilibrium.<sup>3</sup> Oxidative stress is linked to aging and a host of diseases where age is a risk factor, including cancer<sup>4–6</sup> and neurodegenerative Alzheimer's and Parkinson's diseases.<sup>6–8</sup> However, whereas ROS can be damaging when uncontrolled, they also have the potential to be used for beneficial biological activities ranging from immune response to cell signaling.<sup>9–20</sup> At the cellular level, the delicate balance between oxidative stress and signaling is

influenced by the chemistry of a particular ROS or set of ROS, as they are not generated in isolation of one another and can often interconvert and undergo further reactions to produce other ROS metabolites.<sup>3,18,21,22</sup> In other words, at any given time a cell is producing a variety of ROS, where each type exerts specific downstream biological effects. As the lifetimes and reactivities of individual classes of ROS can greatly vary,<sup>18</sup> studying multiple ROS simultaneously in a single cell is critical to understanding their discrete roles in complex environments.

Fluorescent probes are well suited to study the generation of specific types of ROS in biological systems, as optical microscopy allows for the use of multiple probes simultaneously in a single specimen as long as spectral overlap is sufficiently minimized.<sup>23–29</sup> In this regard, several new types of indicators

<sup>†</sup> Department of Chemistry.

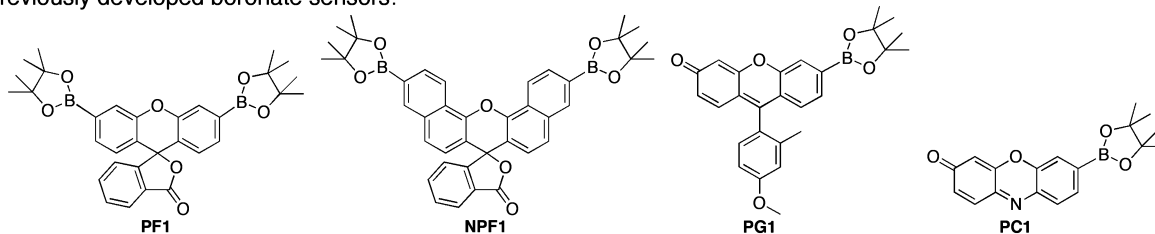
<sup>‡</sup> Howard Hughes Medical Institute.

- (1) Harman, D. *Proc. Natl. Acad. Sci. U.S.A.* **1981**, *78*, 7124–7128.
- (2) Floyd, R. A. *Science* **1991**, *254*, 1597.
- (3) Giorgio, M.; Trinei, M.; Migliaccio, E.; Pelicci, P. G. *Nat. Rev. Mol. Cell. Biol.* **2007**, *8*, 722–728.
- (4) Zhang, W.; Wang, T.; Qin, L.; Gao, H. M.; Wilson, B.; Ali, S. F.; Hong, J. S.; Liu, B. *FASEB J.* **2004**, *18*, 589–591.
- (5) Finkel, T.; Serrano, M.; Blasco, M. A. *Nature* **2007**, *448*, 767–774.
- (6) Park, L.; Zhou, P.; Pitstick, R.; Capone, C.; Anrather, J.; Norris, E. H.; Younkin, L.; Younkin, S.; Carlson, G.; McEwen, B. S.; Iadecola, C. *Proc. Natl. Acad. Sci. U.S.A.* **2008**, *105*, 1347–1352.
- (7) Andersen, J. K. *Nat. Rev. Neurosci.* **2004**, *S18*–25.
- (8) Barnham, K. J.; Masters, C. L.; Bush, A. I. *Nat. Rev. Drug Discovery* **2004**, *3*, 205–214.
- (9) Sundaresan, M.; Yu, Z. X.; Ferrans, V. J.; Irani, K.; Finkel, T. *Science* **1995**, *270*, 296–299.
- (10) Bae, Y. S.; Kang, S. W.; Seo, M. S.; Baines, I. C.; Tekle, E.; Chock, P. B.; Rhee, S. G. *J. Biol. Chem.* **1997**, *272*, 217–221.

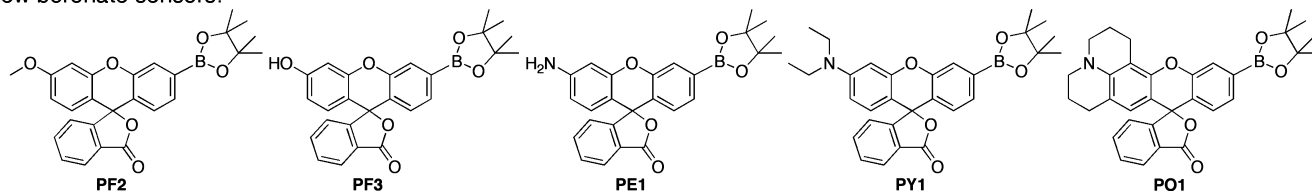
- (11) Avshalumov, M. V.; Rice, M. E. *Proc. Natl. Acad. Sci. U.S.A.* **2003**, *100*, 11729–11734.
- (12) Lambeth, J. D. *Nat. Rev. Immunol.* **2004**, *4*, 181–189.
- (13) Rhee, S. G. *Science* **2006**, *312*, 1882–1883.
- (14) Stone, J. R.; Yang, S. *Antioxid. Redox Signal.* **2006**, *8*, 243–270.
- (15) Miller, E. W.; Chang, C. J. *Curr. Opin. Chem. Biol.* **2007**, *11*, 620–625.
- (16) Miller, E. W.; Tulyathan, O.; Isacoff, E. Y.; Chang, C. J. *Nat. Chem. Biol.* **2007**, *3*, 263–267.
- (17) Veal, E. A.; Day, A. M.; Morgan, B. A. *Mol. Cell* **2007**, *26*, 1–14.
- (18) Winterbourn, C. C. *Nat. Chem. Biol.* **2008**, *4*, 278–286.
- (19) Poole, L. B.; Nelson, K. J. *Curr. Opin. Chem. Biol.* **2008**, *12*, 18–24.
- (20) Paulsen, C. E.; Carroll, K. S. *ACS Chem. Biol.* **2010**, *5*, 47–62.
- (21) Murphy, M. P. *Biochem. J.* **2009**, *417*, 1–13.
- (22) Dickinson, B. C.; Srikun, D.; Chang, C. J. *Curr. Opin. Chem. Biol.* **2010**, *14*, 50–56.
- (23) Shaner, N. C.; Steinbach, P. A.; Tsien, R. Y. *Nat. Meth.* **2005**, *2*, 905–909.

Scheme 1. Boronate-Based H<sub>2</sub>O<sub>2</sub>-Specific Fluorescent Indicators

Previously developed boronate sensors:



New boronate sensors:



have been reported for the detection of nitric oxide (NO),<sup>15,30–36</sup> peroxyxynitrite,<sup>37,38</sup> and nitrate stress,<sup>39</sup> as well as superoxide,<sup>40–43</sup> singlet oxygen,<sup>44,45</sup> ozone,<sup>46</sup> H<sub>2</sub>O<sub>2</sub>,<sup>16,47–65</sup> hypochlorous acid,<sup>66,67</sup> highly reactive oxygen species (hROS),<sup>68–70</sup> and general redox events.<sup>71–84</sup> In terms of H<sub>2</sub>O<sub>2</sub> detection, we previously described the design, synthesis, and characterization of Peroxyfluor-1 (PF1, Scheme 1),<sup>51</sup> a novel probe for H<sub>2</sub>O<sub>2</sub> in which two H<sub>2</sub>O<sub>2</sub>-mediated boronate deprotections yield the highly fluorescent dye molecule fluorescein. Owing to its chemospecific deprotection mechanism, PF1 and related bisboronate derivatives exhibit high selectivity for H<sub>2</sub>O<sub>2</sub> over other ROS and can respond to changes in H<sub>2</sub>O<sub>2</sub> fluxes at oxidative stress levels.<sup>53,58,62</sup> To maintain H<sub>2</sub>O<sub>2</sub> specificity while increasing sensitivity to image H<sub>2</sub>O<sub>2</sub> produced at low signaling levels, we devised the single boronate caged probes Peroxy Green 1 (PG1, Scheme 1) and Peroxy Crimson 1 (PC1, Scheme 1).<sup>16</sup> Green-fluorescent PG1 was capable of visualizing endogenous H<sub>2</sub>O<sub>2</sub> generation in both A431 cells and primary neurons upon epidermal growth factor (EGF) stimulation, but red-fluorescent PC1 was not responsive enough to detect peroxide bursts at these basal levels. Because the most common types of fluorescent reporters utilize GFP, fluorescein, or related green-colored fluorophores that overlap and are thus incompatible with PG1 for multicolor imaging experiments, we sought to address this shortcoming by expanding the available palette of colors for chemospecific peroxide imaging at low cell signaling levels. We now report a new series of monoboronate probes that respond to H<sub>2</sub>O<sub>2</sub> over a range of rationally tunable visible excitation and emission wavelengths (Scheme 1). Three of these derivatives, Peroxyfluor-3 (PF3), Peroxy Yellow 1 (PY1), and Peroxy Orange 1 (PO1), are sensitive enough to image H<sub>2</sub>O<sub>2</sub> signals produced in RAW 264.7 macrophages and A431 cells during immune response and growth factor stimulation, respectively. Moreover, dual-color imaging experiments using PO1 along with the green-fluorescent highly reactive oxygen species (hROS) probe APF allows for selective discrimination between changes in H<sub>2</sub>O<sub>2</sub> and hypochlorous acid (HOCl) levels in macrophages, as well as identification of phagosomes that produce H<sub>2</sub>O<sub>2</sub> and/or hROS during an endogenous immune response.

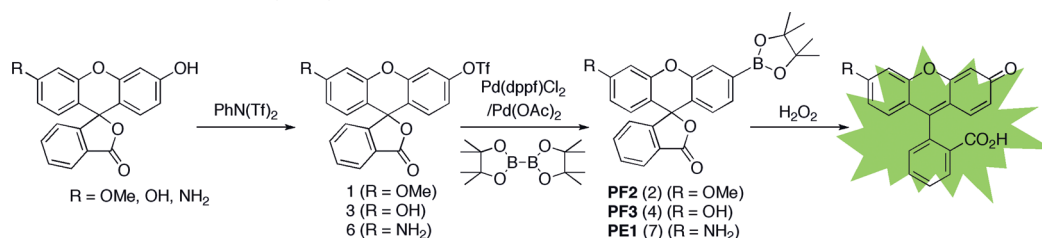
## Results and Discussion

**Design and Synthesis of a Palette of Monoboronate Fluorescent Probes for Hydrogen Peroxide Based on Fluorescein and Rhodol Scaffolds.** The original Tokyo Green fluorophore scaffold utilized for PG1, although functional in many ways, is limited to green

emission profiles. We therefore turned our attention to fluorescein and rhodol dyes that allow us to rationally expand the palette of excitation and emission colors throughout the visible

- (24) Giepmans, B. N. G.; Adams, S. R.; Ellisman, M. H.; Tsien, R. Y. *Science* **2006**, *312*, 217–224.
- (25) Soh, N. *Anal. Bioanal. Chem.* **2006**, *386*, 532–543.
- (26) Domaille, D. W.; Que, E. L.; Chang, C. J. *Nat. Chem. Biol.* **2008**, *4*, 168–175.
- (27) Terai, T.; Nagano, T. *Curr. Opin. Chem. Biol.* **2008**, *12*, 515–521.
- (28) Lavis, L. D.; Raines, R. T. *ACS Chem. Biol.* **2008**, *3*, 142–155.
- (29) Laughlin, S. T.; Bertozzi, C. R. *Proc. Natl. Acad. Sci. U.S.A.* **2009**, *106*, 12–17.
- (30) Kojima, H.; Nakatsubo, N.; Kikuchi, K.; Kawahara, S.; Kirino, Y.; Nagoshi, H.; Hirata, Y.; Nagano, T. *Anal. Chem.* **1998**, *70*, 2446–2453.
- (31) Kojima, H.; Hirotani, M.; Nakatsubo, N.; Kikuchi, K.; Urano, Y.; Higuchi, T.; Hirata, Y.; Nagano, T. *Anal. Chem.* **2001**, *73*, 1967–1973.
- (32) Gabe, Y.; Urano, Y.; Kikuchi, K.; Kojima, H.; Nagano, T. *J. Am. Chem. Soc.* **2004**, *126*, 3357–3367.
- (33) Sasaki, E.; Kojima, H.; Nishimatsu, H.; Urano, Y.; Kikuchi, K.; Hirata, Y.; Nagano, T. *J. Am. Chem. Soc.* **2005**, *127*, 3684–3685.
- (34) Lim, M. H.; Xu, D.; Lippard, S. J. *Nat. Chem. Biol.* **2006**, *2*, 375–380.
- (35) Lim, M. H.; Lippard, S. J. *Acc. Chem. Res.* **2007**, *40*, 41–51.
- (36) McQuade, L. E.; Lippard, S. J. *Curr. Opin. Chem. Biol.* **2010**, *14*, 43–49.
- (37) Yang, D.; Wang, H. L.; Sun, Z. N.; Chung, N. W.; Shen, J. G. *J. Am. Chem. Soc.* **2006**, *128*, 6004–6005.
- (38) Sun, Z. N.; Wang, H. L.; Liu, F. Q.; Chen, Y.; Tam, P. K. H.; Yang, D. *Org. Lett.* **2009**, *11*, 1887–1890.
- (39) Ueno, T.; Urano, Y.; Kojima, H.; Nagano, T. *J. Am. Chem. Soc.* **2006**, *128*, 10640–10641.
- (40) Maeda, H.; Yamamoto, K.; Nomura, Y.; Kohno, I.; Hafsi, L.; Ueda, N.; Yoshida, S.; Fukuda, M.; Fukuyasu, Y.; Yamauchi, Y. *J. Am. Chem. Soc.* **2005**, *127*, 68–69.
- (41) Robinson, K. M.; Janes, M. S.; Pehar, M.; Monette, J. S.; Ross, M. F.; Hagen, T. M.; Murphy, M. P.; Beckman, J. S. *Proc. Natl. Acad. Sci. U.S.A.* **2006**, *103*, 15038–15043.
- (42) Xu, K.; Liu, X.; Tang, B.; Yang, G.; Yang, Y.; An, L. *Chem.—Eur. J.* **2007**, *13*, 1411–1416.
- (43) Xu, K.; Liu, X.; Tang, B. *ChemBioChem* **2007**, *8*, 453–458.
- (44) Umezawa, N.; Tanaka, K.; Urano, Y.; Kikuchi, K.; Higuchi, T.; Nagano, T. *Angew. Chem., Int. Ed.* **1999**, *38*, 2899–2901.
- (45) Song, B.; Wang, G.; Tan, M.; Yuan, J. *J. Am. Chem. Soc.* **2006**, *128*, 13442–13450.
- (46) Garner, A. L.; St Croix, C. M.; Pitt, B. R.; Leikauf, G. D.; Ando, S.; Koide, K. *Nat. Chem.* **2009**, *1*, 316–321.
- (47) Wolfbeis, O. S.; Dürkop, A.; Wu, M.; Lin, Z. *Angew. Chem., Int. Ed.* **2002**, *41*, 4495–4498.
- (48) Meng, O.; Lin, W. Z. *Angew. Chem., Int. Ed.* **2002**, *41*, 4495–4498.
- (49) Onoda, M.; Uchiyama, S.; Endo, A.; Tokuyama, H.; Santa, T.; Imai, K. *Org. Lett.* **2003**, *5*, 1459–1461.
- (50) Lo, L. C.; Chu, C. Y. *Chem. Commun.* **2003**, 2728–2729.
- (51) Chang, M. C. Y.; Pralle, A.; Isacoff, E. Y.; Chang, C. J. *J. Am. Chem. Soc.* **2004**, *126*, 15392–15393.

Scheme 2. Synthesis and Activation of PF2, PF3, and PE1



region by altering oxygen or nitrogen substituents on the 2' position of the xanthene core (Scheme 1). Schemes 2 and 3 outline synthetic routes to a family of five new monoboronate probes for chemoselective H<sub>2</sub>O<sub>2</sub> detection. Two of these probes are based on green methoxyfluorescein (Peroxyfluor-2, PF2) and fluorescein (Peroxyfluor-3, PF3) platforms, whereas the other three reporters feature rhodol derivatives made from aminophenol (Peroxy Emerald 1, PE1), diethylaminophenol (Peroxy Yellow 1, PY1), and julolidine (Peroxy Orange 1, PO1) building blocks. Briefly, treatment of the parent dyes with *N*-phenyl

bis(trifluoromethanesulfonamide) affords the corresponding triflate derivatives, and palladium-mediated coupling with bis(pinacolato)diboron furnishes the final boronate-protected products. PF3 was then acetylated with acetic anhydride to increase cell permeability, where the acetyl functionality should be removed by nonspecific esterases once inside the cytoplasm to reveal PF3. We anticipate that this modular synthetic strategy should be applicable to a wide variety of scaffolds and note complementary synthetic methods for C–N and C–O bond formation that have been reported in the recent literature,<sup>85–92</sup> as well as a triphenylphosphonium-capped piperazine rhodol for mitochondrial targeting.<sup>61</sup>

#### Spectroscopic Properties and Responses to Hydrogen Peroxide.

We evaluated the spectral properties and H<sub>2</sub>O<sub>2</sub> responses of the new monoboronate dyes in aqueous media buffered to physiological pH (20 mM HEPES buffer, pH 7); data are provided in Table 1. The methoxy and boronate groups on PF2 force it to adopt a closed lactone form that is nonfluorescent and displays no absorption features in the visible region. The other four dyes each feature one prominent absorbance band in the visible region with weak but measurable fluorescence. The addition of H<sub>2</sub>O<sub>2</sub> triggers a marked increase in fluorescence intensity for all five probes (Figure 1, S1) with available emission colors spanning from green to yellow to orange. As expected because of their common boronate switch, the fluorescein and rhodol reporters respond with good selectivity to H<sub>2</sub>O<sub>2</sub> over a variety of biologically relevant ROS, including superoxide, NO, hypochlorite, and *tert*-butyl hydroperoxide, as well as hydroxyl and *tert*-butoxy radicals (Figure 2). Kinetics measurements of the H<sub>2</sub>O<sub>2</sub>-mediated boronate deprotections were performed under

(52) Maeda, H.; Fukuyasu, Y.; Yoshida, S.; Fukuda, M.; Saeki, K.; Matsuno, H.; Yamauchi, Y.; Yoshida, K.; Hirata, K.; Miyamoto, K. *Angew. Chem., Int. Ed.* **2004**, *43*, 2389–2391.

(53) Miller, E. W.; Albers, A. E.; Pralle, A.; Isacoff, E. Y.; Chang, C. J. *J. Am. Chem. Soc.* **2005**, *127*, 16652–16659.

(54) Kozhevnikov, V. N.; Mandl, C.; Miltschitzky, S.; Duerkop, A.; Wolfbeis, O. S.; Koenig, B. *Inorg. Chim. Acta* **2005**, *358*, 2445–2448.

(55) Soh, N.; Sakawaki, O.; Makihara, K.; Odo, Y.; Fukaminato, T.; Kawai, T.; Irie, M.; Imato, T. *Bioorg. Med. Chem. Lett.* **2005**, *13*, 1131–1139.

(56) Onoda, M.; Tokuyama, H.; Uchiyama, S.; Mawatari, K.; Santa, T.; Kaneko, K.; Imai, K.; Nakagomi, K. *Chem. Commun.* **2005**, 2005, 1848–1850.

(57) Belousov, V. V.; Fradkov, A. F.; Lukyanov, K. A.; Staroverov, D. B.; Shakhbazov, K. S.; Tersikh, A. V.; Lukyanov, S. *Nat. Methods* **2006**, *3*, 281–286.

(58) Albers, A. E.; Okreglak, V. S.; Chang, C. J. *J. Am. Chem. Soc.* **2006**, *128*, 9640–9641.

(59) Lee, D.; Khaja, S.; Velasquez-Castano, J. C.; Dasari, M.; Sun, C.; Petros, J.; Taylor, W. R.; Murthy, N. *Nat. Mater.* **2007**, *6*, 765–769.

(60) Srikun, D.; Miller, E. W.; Domaille, D. W.; Chang, C. J. *J. Am. Chem. Soc.* **2008**, *130*, 4596–4597.

(61) Dickinson, B. C.; Chang, C. J. *J. Am. Chem. Soc.* **2008**, *130*, 9638–9639.

(62) Albers, A. E.; Dickinson, B. C.; Miller, E. W.; Chang, C. J. *Bioorg. Med. Chem. Lett.* **2008**, *18*, 5948–5950.

(63) Xu, K.; Liu, F.; Wang, H.; Wang, S.; Wang, L.; Tang, B. *Sci. China, Ser. B* **2009**, *52*, 734–740.

(64) Du Y, L.; Ni Y, N.; Li, M.; Wang, B. *Tetrahedron Lett.* **2010**, *51*, 1152–1154.

(65) Srikun, D.; Albers, A. E.; Nam, C. I.; Ivarone, A. T.; Chang, C. J. *J. Am. Chem. Soc.* **2010**, *132*, 4455–4465.

(66) Kenmoku, S.; Urano, Y.; Kojima, H.; Nagano, T. *J. Am. Chem. Soc.* **2007**, *129*, 7313–7318.

(67) Sun, Z. N.; Liu, F. Q.; Chen, Y.; Tam, P. K. H.; Yang, D. *Org. Lett.* **2008**, *10*, 2171–2174.

(68) Setsukinai, K.; Urano, Y.; Kakinuma, K.; Majima, H. J.; Nagano, T. *J. Biol. Chem.* **2003**, *278*, 3170–3175.

(69) Koide, Y.; Urano, Y.; Kenmoku, S.; Kojima, H.; Nagano, T. *J. Am. Chem. Soc.* **2007**, *129*, 10324–10325.

(70) Panizzi, P.; Nahrendorf, M.; Wildgruber, M.; Waterman, P.; Figueiredo, J. L.; Aikawa, E.; McCarthy, J.; Weissleder, R.; Hilderbrand, S. A. *J. Am. Chem. Soc.* **2009**, *131*, 15739–15744.

(71) Hempel, S. L.; Buettner, G. R.; O'Malley, Y. Q.; Wessels, D. A.; Flaherty, D. M. *Free Radical Biol. Med.* **1999**, *27*, 146–159.

(72) Østergaard, H.; Henriksen, A.; Hansen, F. G.; Winther, J. R. *EMBO J.* **2001**, *20*, 5853–5863.

(73) Hanson, G. T.; Aggeler, R.; Oglesbee, D.; Cannon, M.; Capaldi, R. A.; Tsien, R. Y.; Remington, S. J. *J. Biol. Chem.* **2004**, *279*, 13044–13053.

(74) Cline, D. J.; Thorpe, C.; Schneider, J. P. *Anal. Biochem.* **2004**, *325*, 144–150.

(75) Lee, K.; Dzubeck, V.; Latshaw, L.; Schneider, J. P. *J. Am. Chem. Soc.* **2004**, *126*, 13616–13617.

(76) Cannon, M. B.; Remington, S. J. *Protein Sci.* **2006**, *15*, 45–57.

(77) Miller, E. W.; Bian, S. X.; Chang, C. J. *J. Am. Chem. Soc.* **2007**, *129*, 3458–3459.

(78) Ahn, Y. H.; Lee, J. S.; Chang, Y. T. *J. Am. Chem. Soc.* **2007**, *129*, 4510–4511.

(79) Wang, W.; Fang, H.; Groom, L.; Cheng, A.; Zhang, W.; Liu, J.; Wang, X.; Li, K.; Han, P.; Zheng, M. *Cell* **2008**, *134*, 279–290.

(80) Gutscher, M.; Pauleau, A. L.; Marty, L.; Brach, T.; Wabnitz, G. H.; Samstag, Y.; Meyer, A. J.; Dick, T. P. *Nat. Methods* **2008**, *5*, 553–560.

(81) Banerjee, S.; Kar, S.; Perez, J. M.; Santra, S. *J. Phys. Chem. C* **2009**, *113*, 9659–9663.

(82) Shao, N.; Jin, J.; Wang, H.; Zheng, J.; Yang, R.; Chan, W.; Abliz, Z. *J. Am. Chem. Soc.* **2009**, *132*, 725–736.

(83) Kundu, K.; Knight, S. F.; Willett, N.; Lee, S.; Taylor, W. R.; Murthy, N. *Angew. Chem., Int. Ed.* **2009**, *48*, 299–303.

(84) Oshiki, D.; Kojima, H.; Terai, T.; Arita, M.; Hanaoka, K.; Urano, Y.; Nagano, T. *J. Am. Chem. Soc.* **2010**, *132*, 2795–2801.

(85) Burdette, S. C.; Lippard, S. J. *Inorg. Chem.* **2002**, *41*, 6816–6823.

(86) Clark, M. A.; Duffy, K.; Tibrewala, J.; Lippard, S. J. *Org. Lett.* **2003**, *5*, 2051–2054.

(87) Woodroffe, C. C.; Lim, M. H.; Bu, W.; Lippard, S. J. *Tetrahedron* **2005**, *61*, 3097–3105.

(88) Hilderbrand, S. A.; Weissleder, R. *Tetrahedron Lett.* **2007**, *48*, 4383–4385.

(89) Wu, L.; Burgess, K. *Org. Lett.* **2008**, *10*, 1779–1782.

(90) Li, J.; Yao, S. Q. *Org. Lett.* **2008**, *11*, 405–408.

(91) Li, J.; Hu, M.; Yao, S. Q. *Org. Lett.* **2009**, *11*, 3008–3011.

(92) Peng, T.; Yang, D. *Org. Lett.* **2010**, *12*, 496–499.



Scheme 3. Synthesis and Activation of PY1 and PO1

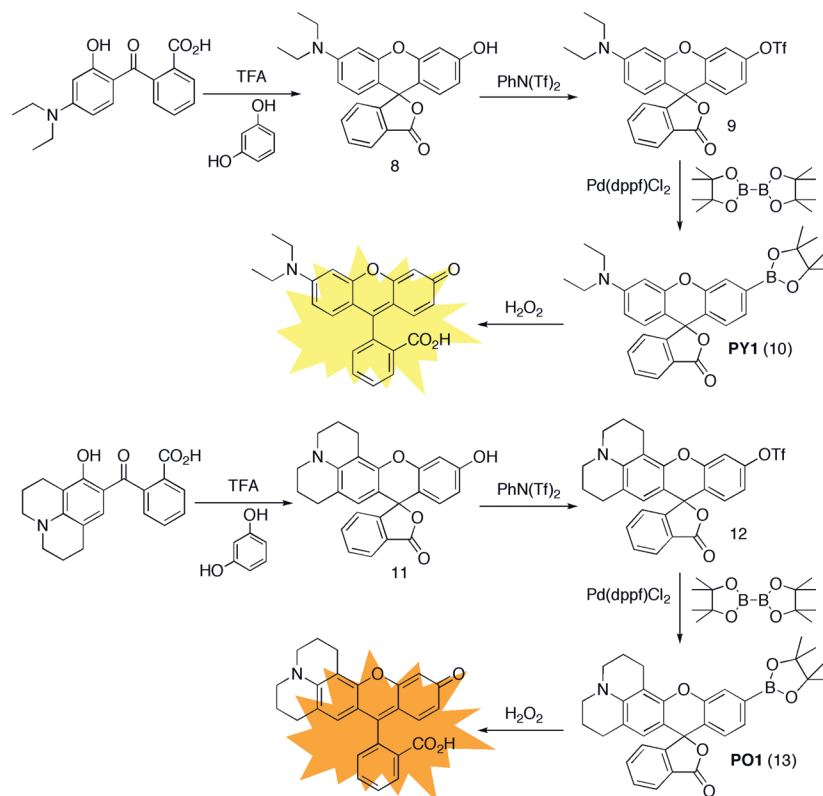


**Table 1.** Spectroscopic Properties of PF2, PF3, PE1, PY1, and PO1 Acquired at 25 °C in 20 mM HEPES, pH 7 (Fluorescein Reported in 0.1 M NaOH<sup>104</sup>)

	Boronate form				Phenol form				$k$ ( $\times 10^{-3} \text{ s}^{-1}$ )
	$\lambda_{\text{abs}}$ (nm)	$\epsilon$ ( $\text{M}^{-1} \text{ cm}^{-1}$ )	$\lambda_{\text{em}}$ (nm)	$\phi$	$\lambda_{\text{abs}}$ (nm)	$\epsilon$ ( $\text{M}^{-1} \text{ cm}^{-1}$ )	$\lambda_{\text{em}}$ (nm)	$\phi$	
PF2	n/a	n/a	n/a	n/a	475	28 600	511	0.27	4.7(1)
PF3	454	24 000	521	0.10	492	88 000	515	0.94	3.8(1)
PE1	480	16 400	519	0.30	491	51 200	514	0.93	8.1(1)
PY1	494	16 200	558	0.01	519	48 900	548	0.12	3.7(1)
PO1	507	13 900	574	0.07	540	29 300	565	0.46	5.2(1)

pseudo-first-order conditions (5  $\mu\text{M}$  dye, 10 mM  $\text{H}_2\text{O}_2$ ), giving observed rate constants ranging from  $k = 3.7(1)$  to  $8.1(1) \times 10^{-3} \text{ s}^{-1}$ . These data provide further evidence that  $\text{H}_2\text{O}_2$ -triggered conversion of boronates to phenols is a robust and versatile methodology for reaction-based  $\text{H}_2\text{O}_2$  detection.

**Fluorescence Detection of  $\text{H}_2\text{O}_2$  in Living Cells in Situations of Oxidative Stress.** With data establishing that all five monoboronate reporters selectively respond to  $\text{H}_2\text{O}_2$  in aqueous solution, we turned our attention to assessing their performance in live-cell imaging assays. Incubation of live A431 cells with 10  $\mu\text{M}$  PF2, 5  $\mu\text{M}$  PF3-Ac, 5  $\mu\text{M}$  PY1, or 5  $\mu\text{M}$  PO1 for 40 min at 37 °C results in low levels of intracellular fluorescence as determined by scanning confocal microscopy measurements (Figure 3a,d,g,j), and addition of 100  $\mu\text{M}$   $\text{H}_2\text{O}_2$  to these dye-loaded cells for 20 min at 37 °C triggers increases in green, yellow, or orange intracellular fluorescence (Figure 3b,e,h,k). PE1 does not show a turn-on response to  $\text{H}_2\text{O}_2$  in cells under similar conditions owing to high background staining. Further brightfield transmission and nuclear staining experiments confirm that the cells are viable throughout the imaging assays (Figures S2, S3). These experiments demonstrate that four of the probes, PF2, PF3-Ac, PY1, and PO1, are cell-

permeable and nontoxic as well as capable of detecting elevations in  $\text{H}_2\text{O}_2$  levels under oxidative stress conditions. The excitation wavelengths of this series of reagents align well with the 488 nm (PF2, PF3-Ac), 514 nm (PY1), and 543 nm (PO1) laser lines commonly used for light microscopy.

**Fluorescence Detection of  $\text{H}_2\text{O}_2$  at Signaling Levels upon Immune or Growth Factor Stimulation.** We next tested whether the monoboronate probes were sensitive enough to detect  $\text{H}_2\text{O}_2$  produced at low signaling levels upon physiological stimulation. Initial experiments focused on macrophages, which fight off infections by engulfing pathogens and using NADPH oxidase (Nox) and associated proteins to produce  $\text{H}_2\text{O}_2$  and other ROS to alleviate the threat.<sup>12,18</sup> We utilized RAW264.7 macrophages, which are estimated to produce low micromolar levels of  $\text{H}_2\text{O}_2$  upon stimulation with phorbol myristate acetate (PMA),<sup>93–95</sup> as a cell line model for  $\text{H}_2\text{O}_2$ -mediated immune response. RAW264.7 cells loaded with 10  $\mu\text{M}$  PF2, 5  $\mu\text{M}$  PF3-Ac, 5  $\mu\text{M}$  PY1, or 5  $\mu\text{M}$  PO1 for 60 min at 37 °C show low levels of intracellular fluorescence (Figure 4a,e,i,m). Upon stimulation of probe-loaded cells with PMA for 40 min at 37 °C to induce an immune response, we observe bright, punctate fluorescent patterns corresponding to phagocytic vesicles (Figure 4b,f,j,n), showing that these reporters can visualize endogenous production of  $\text{H}_2\text{O}_2$  under conditions of immune signaling. We confirmed cell viability during live-cell imaging using a combination of brightfield transmission and nuclear staining experiments (Figures S4, S5).

(93) Wrona, M.; Patel, K.; Wardman, P. *Free Radical Biol. Med.* **2005**, *38*, 262–270.

(94) Li, H.; Li, Q.; Wang, X.; Xu, K.; Chen, Z.; Gong, X.; Liu, X.; Tong, L.; Tang, B. *Anal. Chem.* **2009**, *81*, 2193–2198.

(95) Gong, X.; Li, Q.; Xu, K.; Liu, X.; Li, H.; Chen, Z.; Tong, L.; Tang, B.; Zhong, H. *Electrophoresis* **2009**, *30*, 1983–1990.

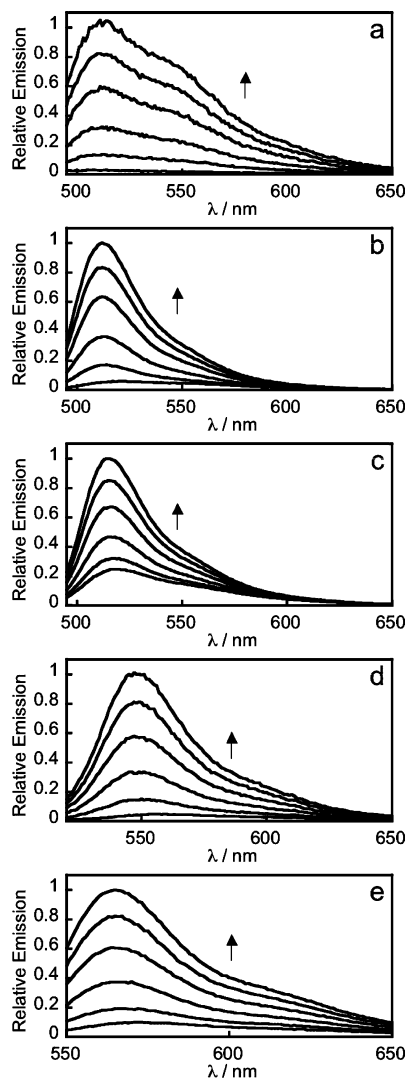


**Figure 1.** Fluorescence turn-on response of 5  $\mu\text{M}$  PF2 (a), PF3 (b), PE1 (c), PY1 (d), or PO1 (e) to  $\text{H}_2\text{O}_2$ . Data were acquired at 25  $^\circ\text{C}$  in 20 mM HEPES, pH 7, with excitation at  $\lambda = 488$  nm for PF2 and PF3,  $\lambda = 490$  nm for PE1,  $\lambda = 514$  nm for PY1, and  $\lambda = 540$  nm for PO1. Emission was collected between 493 and 750 nm for PF2 and PF3, 495 and 750 nm for PE1, 520 and 750 nm for PY1, and 545 and 750 nm for PO1. Time points represent 0, 5, 15, 30, 45, and 60 min after the addition of 100  $\mu\text{M}$   $\text{H}_2\text{O}_2$ . Reactions are not complete at these time points. Full turn-on response of each probe is shown in Figure S1.

We then sought to expand the utility of these fluorescent indicators to image  $\text{H}_2\text{O}_2$  signaling in nonphagocytic systems. In particular, mounting data reveal that Nox proteins used in phagocytic ROS killing are also expressed in a wide variety of nonphagocytic cell types throughout the body and that these enzyme complexes can be activated by ligands such as growth factors and cytokines. We previously showed that A431 cells, which express high levels of epidermal growth factor receptor (EGFR), respond to epidermal growth factor (EGF) stimulation by producing  $\text{H}_2\text{O}_2$  via a Nox/PI3K pathway.<sup>16</sup> Along these lines, A431 cells loaded with 5  $\mu\text{M}$  PF3-Ac, 5  $\mu\text{M}$  PY1, or 5  $\mu\text{M}$  PO1 for 60 min at 37  $^\circ\text{C}$  display modest intracellular fluorescence (Figure 5a,d,g). Treatment of the dye-loaded cells with 500 ng/mL EGF ligand for 40 min at 37  $^\circ\text{C}$  triggers a modest turn-on enhancement in bright green, yellow, or orange intracellular fluorescence compared to unstimulated cells (Figure 5b,e,h) via Nox-generated  $\text{H}_2\text{O}_2$ . Brightfield transmission and

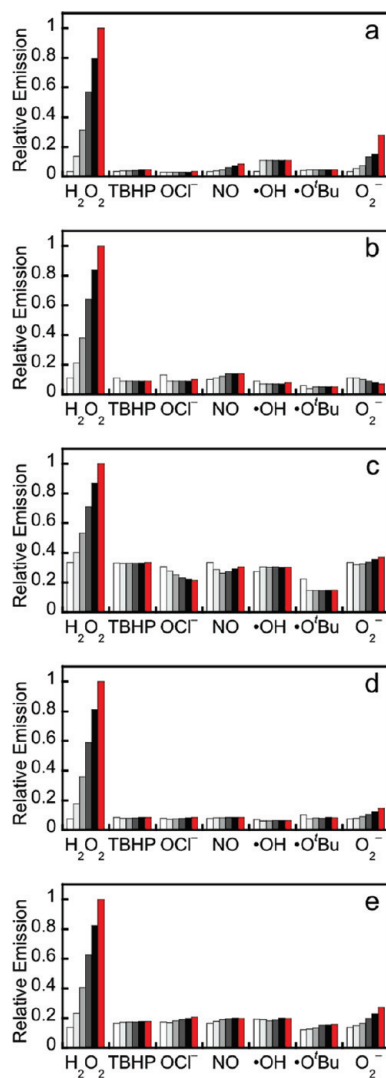


**Figure 2.** Fluorescence responses of 5  $\mu\text{M}$  PF2 (a), PF3 (b), PE1 (c), PY1 (d), and PO1 (e) to various reactive oxygen species (ROS). Bars represent relative responses at 0, 5, 15, 30, 45, and 60 min after addition of each ROS. Data shown are for 200  $\mu\text{M}$  NO and 100  $\mu\text{M}$  for all other ROS. Data were acquired at 25  $^\circ\text{C}$  in 20 mM HEPES, pH 7, with excitation at  $\lambda = 488$  nm for PF2 and PF3,  $\lambda = 490$  nm for PE1,  $\lambda = 514$  nm for PY1, and  $\lambda = 540$  nm for PO1. Emission was collected between 493 and 750 nm for PF2 and PF3, 495 and 750 nm for PE1, 520 and 750 nm for PY1, and 545 and 750 nm for PO1. Time points represent 0, 5, 15, 30, 45, and 60 min after the addition of 100  $\mu\text{M}$   $\text{H}_2\text{O}_2$ . Reactions are not complete at these time points.

nuclear staining measurements confirm that the cells are viable throughout the imaging experiments (Figures S6, S7). Taken together, PF3-Ac, PY1, and PO1 offer a set of green, yellow, and orange dyes that are capable of detecting endogenous bursts of  $\text{H}_2\text{O}_2$  produced for physiological signaling purposes.

**Simultaneous, Dual-Color Imaging of  $\text{H}_2\text{O}_2$  and hROS in Living Cells with Complementary Chemoselective Fluorescent Probes.** Our next goal was to exploit the utility of the newly developed  $\text{H}_2\text{O}_2$ -specific fluorescent indicators with varying emission profiles to image multiple analytes/processes in living cells. In particular, because a given ROS can undergo an array of primary and secondary reactions to produce other classes of ROS molecules, we envisioned using a dual-probe approach to simultaneously visualize  $\text{H}_2\text{O}_2$  and an additional important downstream product of cellular  $\text{H}_2\text{O}_2$  chemistry. We focused on macrophages as a cell model system, as  $\text{H}_2\text{O}_2$  produced by

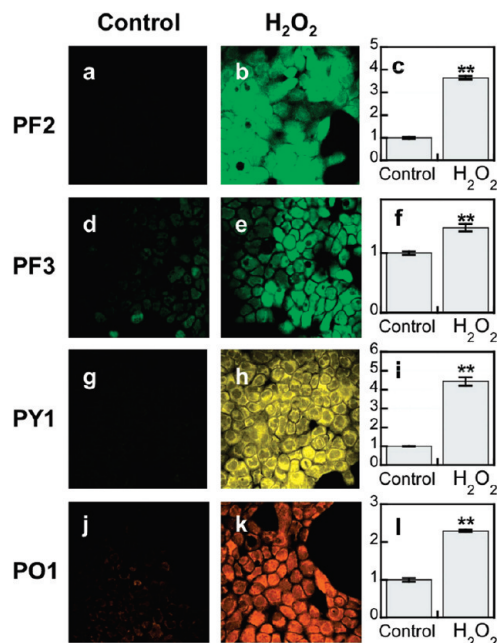


**Figure 3.** Confocal fluorescence images of  $\text{H}_2\text{O}_2$  in live A431 cells under oxidative stress with PF2, PF3-Ac, PY1, and PO1. A431 cells incubated with  $10\ \mu\text{M}$  PF2 for 40 min at  $37\ ^\circ\text{C}$  (a). A431 cells incubated with  $10\ \mu\text{M}$  PF2 for 40 min at  $37\ ^\circ\text{C}$  with  $100\ \mu\text{M}$   $\text{H}_2\text{O}_2$  added for the final 20 min (b) and quantification (c). A431 cells incubated with  $5\ \mu\text{M}$  PF3-Ac for 40 min at  $37\ ^\circ\text{C}$  (d). A431 cells incubated with  $5\ \mu\text{M}$  PF3-Ac for 40 min at  $37\ ^\circ\text{C}$  with  $100\ \mu\text{M}$   $\text{H}_2\text{O}_2$  added for the final 20 min (e) and quantification (f). A431 cells incubated with  $5\ \mu\text{M}$  PY1 for 40 min at  $37\ ^\circ\text{C}$  (g). A431 cells incubated with  $5\ \mu\text{M}$  PY1 for 40 min at  $37\ ^\circ\text{C}$  with  $100\ \mu\text{M}$   $\text{H}_2\text{O}_2$  added for the final 20 min (h) and quantification (i). A431 cells incubated with  $5\ \mu\text{M}$  PO1 for 40 min at  $37\ ^\circ\text{C}$  (j). A431 cells incubated with  $5\ \mu\text{M}$  PO1 for 40 min at  $37\ ^\circ\text{C}$  with  $100\ \mu\text{M}$   $\text{H}_2\text{O}_2$  added for the final 20 min (k) and quantification (l). Data were normalized to controls, and statistical analyses were performed with a two-tailed Student's *t*-test ( $n = 4$ ).  $**P \leq 0.005$  and error bars are  $\pm$  s.e.m.

Nox complexes in these cell types can be converted to HOCl by reaction with heme-dependent myeloperoxidase enzymes.<sup>96–99</sup> For dual-color imaging experiments, we selected APF,<sup>68</sup> a 4-aminophenyl-fluorescein reporter developed by Nagano and co-workers that responds selectively to HOCl and other highly reactive oxygen species (hROS) by an increase in green fluorescence (488 nm excitation, 520 nm emission), along with the  $\text{H}_2\text{O}_2$ -selective probe PO1 that responds in a complementary orange optical window (543 nm excitation, 565 nm emission).

Initial experiments sought to test the ROS specificities of these dyes in a dual-probe/dual-color imaging mode. To this end, RAW264.7 macrophages loaded simultaneously with  $5\ \mu\text{M}$  APF and  $5\ \mu\text{M}$  PO1 for 50 min at  $37\ ^\circ\text{C}$  display low levels of both green and orange fluorescence (Figure 6a,b). In contrast, APF- and PO1-stained cells incubated with  $50\ \mu\text{M}$   $\text{H}_2\text{O}_2$  for 20 min exhibit a selective increase in intracellular orange fluorescence from PO1 without any change in green emission from the APF probe (Figure 6c,d). Moreover, APF- and PO1-loaded cells incubated with  $100\ \mu\text{M}$  HOCl for 20 min give a selective turn-on increase in intracellular green fluorescence from APF without

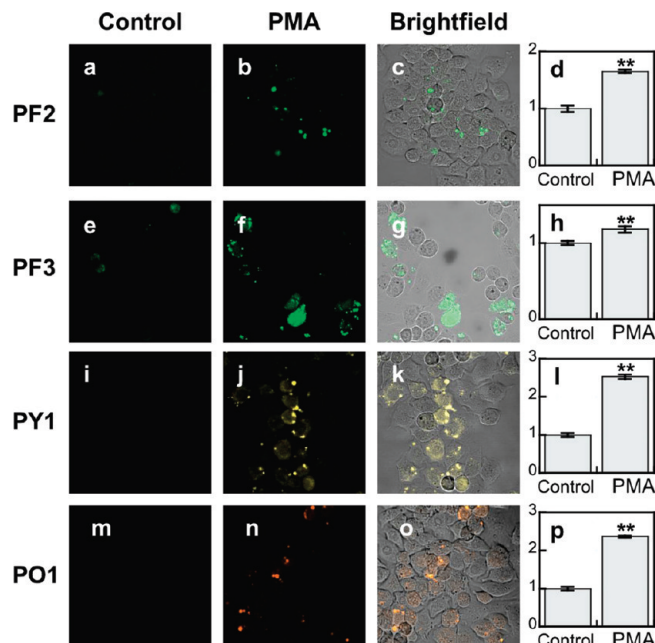


**Figure 4.** Confocal fluorescence images of PMA-induced  $\text{H}_2\text{O}_2$  production in live RAW264.7 macrophages with PF2, PF3-Ac, PY1, and PO1. Macrophages incubated with  $10\ \mu\text{M}$  PF2 for 60 min at  $37\ ^\circ\text{C}$  (a). Macrophages incubated with  $10\ \mu\text{M}$  PF2 for 60 min at  $37\ ^\circ\text{C}$  with  $1\ \mu\text{g}/\text{mL}$  PMA added for the final 40 min (b) with a brightfield overlay (c) and quantification (d). Macrophages incubated with  $5\ \mu\text{M}$  PF3-Ac for 60 min at  $37\ ^\circ\text{C}$  (e). Macrophages incubated with  $5\ \mu\text{M}$  PF3-Ac for 60 min at  $37\ ^\circ\text{C}$  with  $1\ \mu\text{g}/\text{mL}$  PMA added for the final 40 min (f) with a brightfield overlay (g) and quantification (h). Macrophages incubated with  $5\ \mu\text{M}$  PY1 for 60 min at  $37\ ^\circ\text{C}$  (i). Macrophages incubated with  $5\ \mu\text{M}$  PY1 for 60 min at  $37\ ^\circ\text{C}$  with  $1\ \mu\text{g}/\text{mL}$  PMA added for the final 40 min (j) with a brightfield overlay (k) and quantification (l). Macrophages incubated with  $5\ \mu\text{M}$  PO1 for 60 min at  $37\ ^\circ\text{C}$  (m). Macrophages incubated with  $5\ \mu\text{M}$  PO1 for 60 min at  $37\ ^\circ\text{C}$  with  $1\ \mu\text{g}/\text{mL}$  PMA added for the final 40 min (n) with a brightfield overlay (o) and quantification (p). Data were normalized to controls, and statistical analyses were performed with a two-tailed Student's *t*-test ( $n = 4$ ).  $**P \leq 0.005$  and error bars are  $\pm$  s.e.m.

any change in orange emission from the PO1 dye (Figure 6e,f). In all cases, brightfield transmission and nuclear staining measurements confirm reasonable cell viability through the duration of the imaging assays (Figure S8); however the exogenous ROS treatments can cause some toxicity. This set of experiments establishes not only that fluorescence signals arising from green APF and orange PO1 probes can be distinguished by optical microscopy but also that each reporter maintains its chemical selectivity in the presence of one another in living systems.

We then moved on to study endogenously produced ROS bursts using this dual-probe imaging approach. APF- and PO1-loaded macrophages stimulated with  $1\ \mu\text{g}/\text{mL}$  PMA for 20 min display bright, punctate patterns of green and/or orange fluorescence localized to phagosomes, where ROS are generated in response to immune insult (Figures 6g,h, S8). As shown in Figure 7 and Figure S9, we discovered three classes of phagosomes that are characterized by different relative ratios of  $\text{H}_2\text{O}_2$  and hROS fluxes. Specifically, some phagosomes display only PO1-derived orange fluorescence, indicating that  $\text{H}_2\text{O}_2$  production dominates (Figure 7a,b,c,d), whereas other phagosomes show only APF-derived green fluorescence, indicating that most of the phagocytic burst results in formation of hROS (Figure 7e,f,g,h). A third distinct class of phagosomes possesses both green and orange fluorescence signals (Figure 7i,j,k,l) resulting from a combination of phagocytic increases

(96) Hampton, M. B.; Kettle, A. J.; Winterbourn, C. C. *Blood* **1998**, *92*, 3007–3017.

(97) Winterbourn, C. C.; Vissers, M.; Kettle, A. J. *Curr. Opin. Hematol.* **2000**, *7*, 53–58.

(98) Karlsson, A.; Dahlgren, C. *Antioxid. Redox Signal.* **2002**, *4*, 49–60.

(99) van der Veen, B. S.; de Winther, M. P. J.; Heeringa, P.; Augusto, O.; Chen, J. W.; Davies, M.; Ma, X. L.; Malle, E.; Pignatelli, P.; Rudolph, T. *Antioxid. Redox Signal.* **2009**, *11*, 2899–2937.



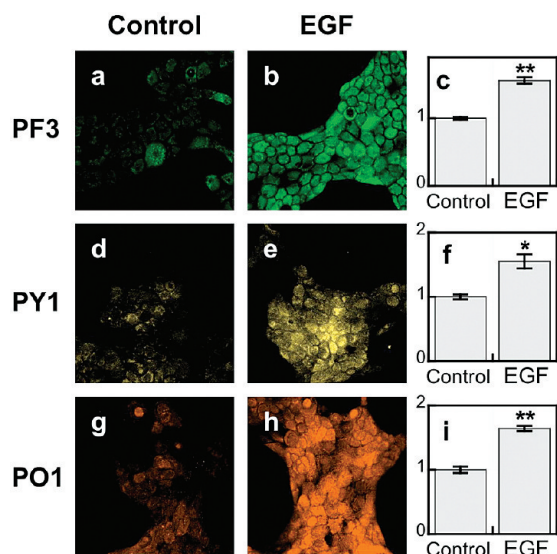


**Figure 5.** Confocal fluorescence images of EGF-induced  $\text{H}_2\text{O}_2$  in live A431 cells with PF3-Ac, PY1, and PO1. A431 cells incubated with  $5 \mu\text{M}$  PF3-Ac for 60 min at  $37^\circ\text{C}$  (a). A431 cells incubated with  $5 \mu\text{M}$  PF3-Ac for 60 min at  $37^\circ\text{C}$  with  $500 \text{ ng/mL}$  EGF added for the final 40 min (b) and quantification (c). A431 cells incubated with  $5 \mu\text{M}$  PY1 for 60 min at  $37^\circ\text{C}$  (d). A431 cells incubated with  $5 \mu\text{M}$  PY1 for 60 min at  $37^\circ\text{C}$  with  $500 \text{ ng/mL}$  EGF added for the final 40 min (e) and quantification (f). A431 cells incubated with  $5 \mu\text{M}$  PO1 for 60 min at  $37^\circ\text{C}$  (g). A431 cells incubated with  $5 \mu\text{M}$  PO1 for 60 min at  $37^\circ\text{C}$  with  $500 \text{ ng/mL}$  EGF added for the final 20 min (h) and quantification (i). Data were normalized to controls, and statistical analyses were performed with a two-tailed Student's *t*-test ( $n = 4$ ).  $*P \leq 0.05$ ;  $**P \leq 0.005$  and error bars are  $\pm$  s.e.m.

in both  $\text{H}_2\text{O}_2$  and hROS. These data establish that the dual-probe approach can reveal chemical differences through simultaneous imaging of discrete classes of ROS molecules.

### Concluding Remarks

To close, we have described the synthesis, properties, and biological applications of a new class of monoboronate fluorescent probes for imaging  $\text{H}_2\text{O}_2$  produced at low signaling levels with a range of varying excitation and emission colors. By rationally tuning substituents on a homologous xanthenone core, we have developed boronate-caged fluorescein and rhodol derivatives for  $\text{H}_2\text{O}_2$  detection with excitation profiles that match well with common 488, 514, and 543 nm lines used for light

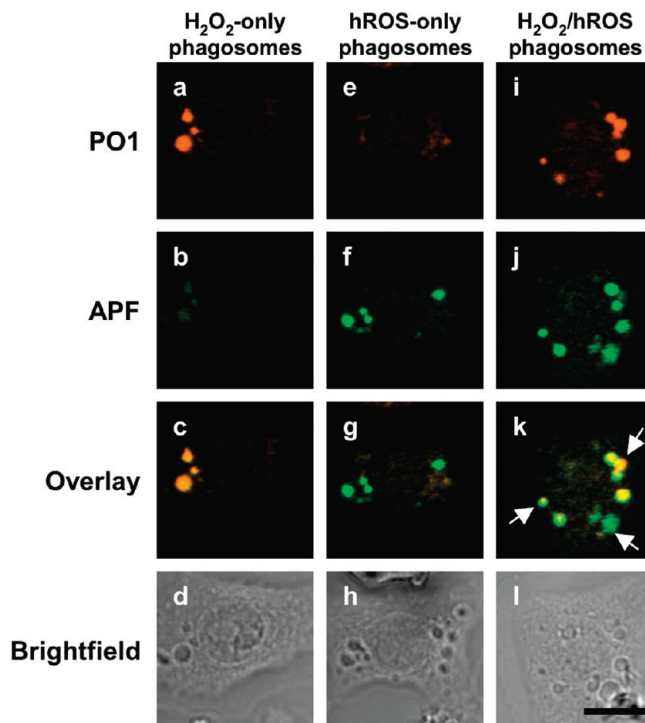


**Figure 7.** Confocal fluorescence images of different types of phagosomes in live RAW264.7 macrophages distinguished by PO1 and APF. A macrophage producing mostly  $\text{H}_2\text{O}_2$  as shown by the PO1 signal (a), APF signal (b), overlay (c), and brightfield (d). A macrophage producing mostly hROS as shown by the PO1 signal (e), APF signal (f), overlay (g), and brightfield (h). A macrophage producing a mixture of  $\text{H}_2\text{O}_2$  phagosomes, hROS phagosomes, and  $\text{H}_2\text{O}_2$  and hROS phagosomes, as shown by the PO1 signal (i), APF signal (j), overlay (k), and brightfield (l).  $10 \mu\text{m}$  scale bar shown.

microscopy. All five probes in this series give a selective turn-on fluorescence response to  $\text{H}_2\text{O}_2$  in aqueous solution buffered to physiological pH with minimal interference from other biologically relevant ROS. Moreover, PF2, PF3-Ac, PY1, and PO1 are capable of visualizing changes in  $\text{H}_2\text{O}_2$  levels in living cells in situations of oxidative stress, and PF3-Ac, PY1, and PO1 can be used to image low levels of  $\text{H}_2\text{O}_2$  produced for signaling purposes upon phagocytic immune or nonphagocytic growth factor stimulation in live samples. Owing to the expanded color palette of  $\text{H}_2\text{O}_2$ -selective probes with sensitivity

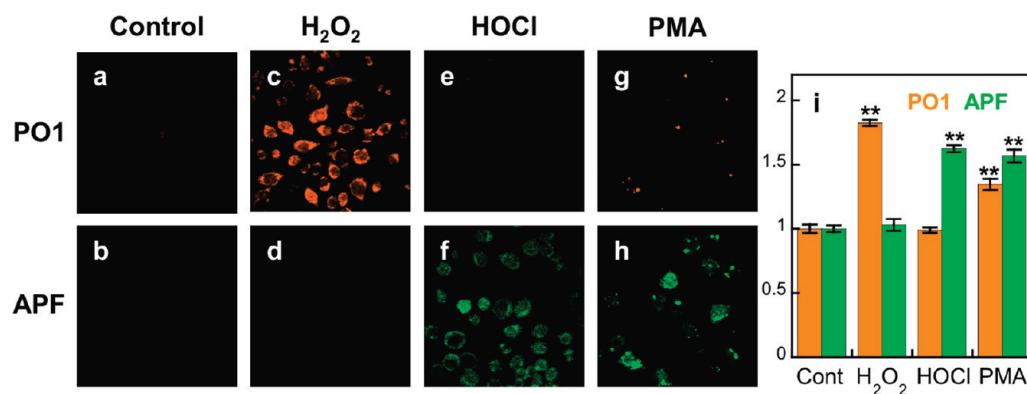


**Figure 6.** Confocal fluorescence images of PMA-induced ROS production in live RAW264.7 macrophages with PO1 and APF simultaneously. Macrophages incubated with  $5 \mu\text{M}$  PO1 and  $5 \mu\text{M}$  APF for 40 min at  $37^\circ\text{C}$  and imaged for PO1 (a) and APF (b). Macrophages incubated with  $5 \mu\text{M}$  PO1 and  $5 \mu\text{M}$  APF for 40 min at  $37^\circ\text{C}$  with  $50 \mu\text{M}$   $\text{H}_2\text{O}_2$  added for the final 20 min and imaged for PO1 (c) and APF (d). Macrophages incubated with  $5 \mu\text{M}$  PO1 and  $5 \mu\text{M}$  APF for 40 min at  $37^\circ\text{C}$  with  $100 \mu\text{M}$  HOCl added for the final 20 min and imaged for PO1 (e) and APF (f). Macrophages incubated with  $5 \mu\text{M}$  PO1 and  $5 \mu\text{M}$  APF for 40 min at  $37^\circ\text{C}$  with  $1 \mu\text{g/mL}$  PMA added for the final 20 min and imaged for PO1 (g) and APF (h). Quantification of a–h (i). Data were normalized to controls, and statistical analyses were performed with a two-tailed Student's *t*-test ( $n = 4$ ).  $**P \leq 0.005$  and error bars are  $\pm$  s.e.m.

to low cell signaling levels, we were able to combine one of our newly synthesized H<sub>2</sub>O<sub>2</sub> probes, PO1, with a complementary green-fluorescent reporter for hROS, APF, for selective discrimination between changes in H<sub>2</sub>O<sub>2</sub> and HOCl levels in live RAW264.7 macrophages by a dual-probe/dual-color imaging approach. Further, we observed that PMA-stimulated macrophages were shown to respond with three discrete types of phagosomes via PO1/APF imaging: those that produced primarily hROS and selectively turned on APF during the phagocytic burst, those that primarily generated H<sub>2</sub>O<sub>2</sub> and caused an increase in PO1 fluorescence, and those that deprotected both PO1 and APF probes and, therefore, possessed an elevated mixture of both H<sub>2</sub>O<sub>2</sub> and hROS during immune signaling. By establishing selective H<sub>2</sub>O<sub>2</sub>-responsive probes with varying emission colors that can be used at low signaling levels, this work greatly expands our ability to study peroxide biology, particularly in conjunction with other reporters for cellular analytes and reaction processes. We are currently pursuing such opportunities in a variety of physiological and disease models, with particular interest in brain and immune systems.

## Experimental Section

**Synthetic Materials and Methods.** All reactions were carried out under a dry nitrogen atmosphere. 2-(4-Diethylamino-2-hydroxybenzoyl)benzoic acid,<sup>100</sup> 8-hydroxy-9-*o*-carboxybenzoyljulolidine,<sup>101</sup> rhodol,<sup>102</sup> and methoxyfluorescein<sup>103</sup> were synthesized according to literature methods. Silica gel P60 (SiliCycle) was used for column chromatography. Analytical thin layer chromatography was performed using SiliCycle 60 F254 silica gel (precoated sheets, 0.25 mm thick). All chemicals were purchased from Sigma-Aldrich (St. Louis, MO) and used as received. <sup>1</sup>H NMR, <sup>13</sup>C NMR, and <sup>31</sup>P NMR spectra were collected in CDCl<sub>3</sub>, (CD<sub>3</sub>)<sub>2</sub>O, or 9:1 CDCl<sub>3</sub>/CD<sub>3</sub>OD (Cambridge Isotope Laboratories, Cambridge, MA) at 25 °C on a Bruker AV-300, AVQ-400, or DRX-500 spectrometer at the College of Chemistry NMR Facility at the University of California, Berkeley. All chemical shifts are reported in the standard δ notation of parts per million using the peak of residual solvent proton signals as an internal reference. High-resolution mass spectral analyses were carried out at the College of Chemistry Mass Spectrometry Facility at the University of California, Berkeley. Low-resolution mass spectral analyses were carried out on an Agilent 6130 LC/MS system (Santa Clara, CA). Microwave reactions were performed using a CEM Intelligent Explorer/Discover (Matthews, NC).

**Methoxyfluorescein Triflate (1).** Methoxyfluorescein (500 mg, 1.45 mmol) and *N*-phenyl bis(trifluoromethanesulfonamide) (2.06 g, 5.78 mmol) were added to a vial and dissolved in 10 mL of dimethylformamide. Diisopropylethylamine (1.22 mL, 7.37 mmol) was then added, and the reaction stirred for 120 min at room temperature. The reaction was then extracted into dichloromethane, washed three times with water, and dried under reduced pressure. Purification by column chromatography (2:1 hexanes/ethyl acetate) yielded **1** as a white solid (440 mg, 63%). <sup>1</sup>H NMR ((CD<sub>3</sub>)<sub>2</sub>O, 400 MHz): δ 8.0 (1H, d, *J* = 7.6 Hz), 7.84 (1H, dt, *J* = 1.2, 7.2 Hz), 7.78 (1H, dt, *J* = 1.2, 7.2 Hz), 7.54 (1H, D, *J* = 2.4 Hz), 7.38 (1H, d, *J* = 7.6 Hz), 7.25 (1H, dd, *J* = 2.4, 8.8 Hz), 7.13 (1H, d, *J* = 8.8 Hz), 7.94 (1H, d, *J* = 2.4 Hz), 6.82 (1H, d, *J* = 8.8 Hz), 6.78

(1H, dd, *J* = 2.4, 8.8 Hz), 3.89 (3H, s). <sup>13</sup>C NMR ((CD<sub>3</sub>)<sub>2</sub>O, 100 MHz): δ 169.2, 162.9, 153.6, 152.9, 152.8, 151.1, 136.6, 131.6, 131.4, 130.1, 127.3, 125.9, 125.0, 121.5, 118.1, 113.6, 111.9, 111.5, 101.73, 56.24. <sup>19</sup>F NMR ((CD<sub>3</sub>)<sub>2</sub>O, 376.5 MHz): δ -73.25. HR-FABMS: calculated for [M<sup>+</sup>] 479.0412, found 479.0426.

**Peroxyfluor-2, PF2 (2).** Compound **1** (150 mg, 0.31 mmol), bis(pinacolato)diboron (120 mg, 0.47 mmol), palladium acetate (63 mg, 0.10 mmol), and cyclo-hexyl JohnPhos (66 mg, 0.20 mmol) were added to a glass vial in an inert atmosphere glovebox and dissolved in 3 mL of dioxane. Diisopropylethylamine (0.31 mL, 1.79 mmol) was then added the vial, and the contents were stirred at room temperature overnight. The contents were then brought out of the box and dried under reduced pressure. Purification by column chromatography (2:1 hexanes/ethyl acetate) afforded PF2 as a white solid (103 mg, 73%). <sup>1</sup>H NMR ((CD<sub>3</sub>)<sub>2</sub>O, 400 MHz): δ 8.02 (1H, d, *J* = 7.6 Hz), 7.79 (1H, t, *J* = 6.8 Hz), 7.74 (1H, t, *J* = 7.2 Hz), 7.66 (1H, s), 7.46 (1H, d, *J* = 8.0 Hz), 7.26 (1H, d, *J* = 7.6 Hz), 6.90 (1H, d, *J* = 4.0 Hz), 6.89 (1H, s), 6.78 (1H, d, *J* = 8.8 Hz), 6.72 (1H, dd, *J* = 2.4, 8.8 Hz), 3.86 (3H, s), 1.35 (12H, s). <sup>13</sup>C NMR ((CD<sub>3</sub>)<sub>2</sub>O, 100 MHz): δ 169.5, 162.6, 154.1, 153.2, 151.6, 136.3, 131.0, 130.4, 130.0, 128.3, 127.2, 125.7, 124.9, 123.8, 123.1, 112.8, 112.1, 106.7, 85.1, 82.7, 56.1, 25.5. HR-FABMS: calculated for [M<sup>+</sup>] 457.1822, found 457.1831.

**Fluorescein Monotriflate (3).** Fluorescein (2.0 g, 5.8 mmol) and *N*-phenyl bis(trifluoromethanesulfonamide) (2.1 g, 5.8 mmol) were added to a dry Schlenk flask and flushed with nitrogen. The reaction contents were dissolved in 15 mL of DMF, and diisopropylethylamine (3.8 mL, 23.1 mmol) was added. After 48 h of stirring of the contents at room temperature, the reaction mixture was acidified with hydrochloric acid, extracted into ethyl acetate, and evaporated under reduced pressure. Purification by column chromatography (1:1 hexanes/ethyl acetate) afforded **3** as a pale yellow solid (1.7 g, 63%). <sup>1</sup>H NMR ((CD<sub>3</sub>)<sub>2</sub>O, 400 MHz): δ 8.01 (1H, d, *J* = 8.0 Hz), 7.81 (1H, dt, *J* = 1.2, 7.6 Hz), 7.75 (1H, dt, *J* = 1.2, 7.6 Hz), 7.50 (1H, d, *J* = 2.4 Hz), 7.36 (1H, d, *J* = 7.6 Hz), 7.21 (1H, dd, *J* = 2.4, 8.8 Hz), 7.09 (1H, d, *J* = 8.8 Hz), 6.81 (1H, d, *J* = 2.4 Hz), 6.72 (1H, d, *J* = 8.8 Hz), 6.68 (1H, dd, *J* = 2.4, 8.8 Hz). <sup>13</sup>C NMR ((CD<sub>3</sub>)<sub>2</sub>O, 100 MHz): δ 168.2, 159.7, 152.6, 152.0, 151.8, 150.0, 135.5, 130.5, 130.3, 129.3, 126.3, 124.8, 124.0, 120.5, 117.0, 113.2, 110.4, 110.0, 102.5, 81.1. <sup>19</sup>F NMR ((CD<sub>3</sub>)<sub>2</sub>O, 376.5 MHz): δ -73.21. HR-FABMS: calculated for [M<sup>+</sup>] 465.0256, found 465.0243.

**Peroxyfluor-3, PF3 (4).** Compound **3** (200 mg, 0.43 mmol), bis(pinacolato)diboron (111 mg, 0.430 mmol), Pd(dppf)Cl<sub>2</sub>·CH<sub>2</sub>Cl<sub>2</sub> (106 mg, 0.130 mmol), potassium acetate (127 mg, 1.29 mmol), and 10 mL of toluene were added to a dry pressure tube in an inert atmosphere glovebox. The pressure tube was then brought out of the box and microwave-heated for 2 h at 110 °C. After the reaction mixture was cooled to room temperature, the contents of the pressure flask were washed into a round-bottom flask with dichloromethane and evaporated to dryness. Purification by column chromatography (1:1 hexanes/ethyl acetate) delivered **4** as a yellow solid (105 mg, 55%). <sup>1</sup>H NMR ((CD<sub>3</sub>)<sub>2</sub>O, 400 MHz): δ 8.00 (1H, d, *J* = 7.6 Hz), 7.76 (1H, t, *J* = 6.8 Hz), 7.70 (1H, t, *J* = 6.8 Hz), 7.64 (1H, s), 7.43 (1H, d, *J* = 7.6 Hz), 7.24 (1H, d, *J* = 7.6 Hz), 6.86 (1H, d, *J* = 8.0 Hz), 6.80 (1H, d, *J* = 2.0 Hz), 6.69 (1H, d, *J* = 8.4 Hz), 6.64 (1H, dd, *J* = 2.0, 8.4 Hz), 1.32 (12H, s). <sup>13</sup>C NMR ((CD<sub>3</sub>)<sub>2</sub>O, 100 MHz): δ 168.7, 159.7, 153.2, 152.2, 151.4, 150.7, 135.3, 130.0, 129.3, 129.1, 127.4, 126.3, 124.7, 123.9, 122.9, 122.2, 112.7, 110.1, 102.6, 84.1, 82.1, 24.3. HR-FABMS: calculated for [M<sup>+</sup>] 443.1676, found 443.1666.

**Peroxyfluor-3 Acetate, PF3-Ac (5).** Compound **4** (33 mg, 0.080 mmol) and cesium carbonate (121 mg, 0.370 mmol) were added to a dry Schlenk tube and dissolved in 3 mL of dry acetonitrile. Acetic anhydride (14 μL, 0.15 mmol) was added, and the reaction stirred at room temperature for 30 min. The contents of the reaction were evaporated under reduced pressure. Purification by column chromatography (3:1 hexanes/ethyl acetate) afforded **5** as a clear film (16 mg, 43%). <sup>1</sup>H NMR (CDCl<sub>3</sub>/10% CD<sub>3</sub>OD, 400 MHz): 8.04

(100) Patel, S. V.; Patel, M. P.; Patel, R. G. *J. Serb. Chem. Soc.* **2005**, *70*, 931–936.

(101) Sauers, R. R.; Husain, S. N.; Piechowski, A. P.; Bird, G. R. *Dyes Pigm.* **1987**, *8*, 35–53.

(102) Whitaker, J. E.; Haugland, R. P.; Ryan, D.; Hewitt, P. C.; Haugland, R. P.; Prendergast, F. G. *Anal. Biochem.* **1992**, *207*, 267–279.

(103) Mughlerli, L.; Burchak, O. N.; Chatelain, F.; Balakirev, M. Y. *Bioorg. Med. Chem. Lett.* **2006**, *16*, 4488–4491.

(104) Heller, C. A.; Henry, R. A.; McLaughlin, B. A.; Bliss, D. E. *J. Chem. Eng. Data* **1974**, *19*, 214–219.



(1H, d,  $J = 6.8$  Hz), 7.75 (1H, s), 6.64 (2H, quintet,  $J = 7.2$  Hz), 4.45 (1H, d,  $J = 7.6$  Hz), 7.14 (1H, d,  $J = 7.2$  Hz), 7.08 (1H, d,  $J = 2.0$  Hz), 6.82 – 6.88 (2H, m), 6.80 (1H, dd,  $J = 2.0, 8.4$  Hz), 2.32 (1H, s), 1.35 (12H, s). HR-FABMS: calculated for  $[M^+]$  485.1772, found 485.1780.

**Aniline Rhodol Triflate (6).** Rhodol (150 mg, 0.46 mmol) and *N*-phenyl bis(trifluoromethanesulfonamide) (250 mg, 0.69 mmol) were added to a glass vial and dissolved in 10 mL of acetonitrile. Diisopropylethylamine (0.23 mL, 1.4 mmol) was added, and the reaction stirred at room temperature for 72 h. The product was then extracted into ethyl acetate, washed once with water, and dried under reduced pressure. Purification by column chromatography (1:1 hexanes/ethyl acetate) yielded **6** as a white solid (49 mg, 23%).  $^1\text{H}$  NMR ( $(\text{CD}_3)_2\text{O}$ , 400 MHz):  $\delta$  7.99 (1H, d,  $J = 7.6$  Hz), 7.80 (1H, t,  $J = 7.6$  Hz), 7.73 (1H, t,  $J = 7.2$  Hz), 7.46 (1H, d,  $J = 2.0$  Hz), 7.33 (1H, d,  $J = 7.6$  Hz), 7.17 (1H, dd,  $J = 2.0, 8.8$  Hz), 7.04 (1H, d,  $J = 8.8$  Hz), 6.60 (1H, s), 6.52 (1H, d,  $J = 8.8$  Hz), 6.48 (1H, d,  $J = 8.4$  Hz).  $^{13}\text{C}$  NMR ( $(\text{CD}_3)_2\text{O}$ , 100 MHz):  $\delta$  168.4, 152.6, 152.2, 152.0, 149.9, 135.4, 130.4, 130.1, 128.7, 126.7, 124.6, 124.0, 120.8, 118.7 (q,  $J = 318$  Hz), 116.6, 112.0, 110.3, 106.1, 99.8, 81.9.  $^{19}\text{F}$  NMR (Acetone, 376.5 MHz):  $\delta$  -73.217. Low-res MS: 464.1.

**Peroxy Emerald 1, PE1 (7).** **6** (49 mg, 0.11 mmol), bis(pinacolato)diboron (27 mg, 0.11 mmol), Pd(dppf) $\text{Cl}_2 \cdot \text{CH}_2\text{Cl}_2$  (26 mg, 0.03 mmol), potassium acetate (31 mg, 0.32 mmol), and 3 mL of toluene were added to a dry pressure tube in an inert atmosphere glovebox. The pressure tube was then brought out of the box and microwave-heated for 4 h at 110 °C. After the reaction cooled to room temperature, the reaction contents were washed into a round-bottom flask with dichloromethane and methanol and dried under reduced pressure. Purification by column chromatography (1:1 hexanes/ethyl acetate) yielded PE1 as a light orange solid (7.0 mg, 15%).  $^1\text{H}$  NMR (Acetone, 400 MHz):  $\delta$  7.99 (1H, d,  $J = 7.6$  Hz), 7.78 (1H, t,  $J = 7.6$  Hz), 7.72 (1H, t,  $J = 7.6$  Hz), 7.62 (1H, s), 7.41 (1H, d,  $J = 7.6$  Hz), 7.26 (1H, d,  $J = 7.6$  Hz), 6.83 (1H, d,  $J = 7.6$  Hz), 6.60 (1H, d,  $J = 2.0$  Hz), 6.52 (1H, d,  $J = 8.8$  Hz), 6.45 (1H, dd,  $J = 2.0, 8.8$  Hz), 1.34 (12H, s).  $^{13}\text{C}$  NMR (Acetone, 100 MHz):  $\delta$  169.6, 154.2, 153.3, 152.1, 151.9, 136.1, 130.8, 129.9, 129.6, 128.3, 127.7, 125.4, 124.9, 123.8, 123.4, 112.4, 107.4, 100.9, 85.0, 83.7, 74.9, 25.2. HR-FABMS: calculated for  $[M^+]$  442.1831, found 442.1820.

**Diethylamino Rhodol (8).** Synthesis adopted from literature.<sup>101</sup> 2-(4-Diethylamino-2-hydroxybenzoyl)benzoic acid (1.26 g, 4.00 mmol) and resorcinol (443 g, 4.0 mmol) were added to a heavy-walled pressure flask and dissolved in 15 mL of trifluoroacetic acid. The reaction contents were heated to 90 °C for 12 h, then cooled to room temperature, and evaporated to dryness. Purification by column chromatography (4.5:4.5:1 dichloromethane/ethyl acetate/methanol) delivered **8** as a red-brown solid (1.2 g, 77% yield).  $^1\text{H}$  NMR ( $\text{CDCl}_3/10\% \text{CD}_3\text{OD}$ , 400 MHz):  $\delta$  8.19 (1H, d,  $J = 7.2$  Hz), 7.59 (2H, quartet,  $J = 7.2$  Hz), 7.11 (1H, d,  $J = 7.2$  Hz), 6.86–6.95 (3H, m), 6.68 (2H, dd,  $J = 2.0, 9.2$  Hz), 6.64 (1H, d,  $J = 2.0$  Hz), 3.44 (4H, q,  $J = 7.2$  Hz), 1.16 (6H, t,  $J = 7.2$  Hz).  $^{13}\text{C}$  NMR ( $\text{CDCl}_3/10\% \text{CD}_3\text{OD}$ , 100 MHz):  $\delta$  163.5, 153.4, 152.4, 150.9, 128.9, 127.3, 126.7, 126.2, 126.0, 124.4, 113.2, 110.0, 109.7, 108.7, 98.6, 92.3, 41.8, 8.3. HR-FABMS: calculated for  $[M^+]$  388.1549, found 388.1546.

**Diethylamino Rhodol Triflate (9).** Compound **8** (500 mg, 1.39 mmol) and *N*-phenyl bis(trifluoromethanesulfonamide) (745 mg, 2.09 mmol) were added to a vial and flushed with nitrogen. The reaction contents were dissolved in 5 mL of DMF, and diisopropylethylamine (691  $\mu\text{L}$ , 4.18 mmol) was added. After 10 min of stirring at room temperature, the product was extracted into ethyl acetate, washed three times with water, and evaporated under reduced pressure. Purification by column chromatography (3:1 hexanes/ethyl acetate) afforded **9** as a light pink solid (440 mg, 61%).  $^1\text{H}$  NMR ( $\text{CDCl}_3/10\% \text{CD}_3\text{OD}$ , 400 MHz):  $\delta$  7.99 (1H, d,  $J = 7.6$  Hz), 7.65 (1H, t,  $J = 7.2$  Hz), 7.60 (1H, t,  $J = 7.2$  Hz), 7.20 (1H, d,  $J = 2.4$  Hz), 7.17 (1H, d,  $J = 7.6$  Hz), 6.90 (1H, dd,  $J =$

2.4, 8.8 Hz), 6.84 (1H, d,  $J = 8.8$  Hz), 6.54 (1H, d,  $J = 9.2$  Hz), 6.44 (1H, d,  $J = 2.4$  Hz), 6.36 (1H, dd,  $J = 2.4, 8.8$  Hz), 3.31 (4H, q,  $J = 7.2$  Hz), 1.11 (6H, t,  $J = 7.2$  Hz).  $^{13}\text{C}$  NMR ( $\text{CDCl}_3/10\% \text{CD}_3\text{OD}$ , 100 MHz):  $\delta$  169.5, 152.5, 152.4, 152.4, 149.8, 149.8, 135.3, 130.0, 129.2, 128.7, 126.7, 125.0, 124.0, 123.4, 120.2, 116.1, 113.8, 110.3, 109.0, 104.1, 97.4, 83.1, 44.4, 12.3.  $^{19}\text{F}$  NMR ( $\text{CDCl}_3/10\% \text{CD}_3\text{OD}$ , 376.5 MHz):  $\delta$  -72.05. HR-FABMS: calculated for  $[M^+]$  520.1042, found 520.1036.

**Peroxy Yellow 1, PY1 (10).** Compound **9** (200 mg, 0.38 mmol), bis(pinacolato)diboron (94 mg, 0.38 mmol), Pd(dppf) $\text{Cl}_2 \cdot \text{CH}_2\text{Cl}_2$  (94 mg, 0.12 mmol), potassium acetate (113 mg, 1.16 mmol), and 3 mL of toluene were added to a dry pressure tube in an inert atmosphere glovebox. The pressure tube was then brought out of the box and microwave-heated for 2 h at 110 °C. After cooling the reaction mixture to room temperature, the contents of the pressure flask were washed into a round-bottom flask with dichloromethane and evaporated to dryness. Purification by column chromatography (4:1 hexanes/ethyl acetate) delivered PY1 as a light tan solid (41 mg, 22%).  $^1\text{H}$  NMR ( $\text{CDCl}_3/10\% \text{CD}_3\text{OD}$ , 400 MHz):  $\delta$  7.98 (1H, d,  $J = 7.6$  Hz), 7.69 (1H, s), 7.62 (1H, t,  $J = 7.2$  Hz), 7.58 (1H, t,  $J = 7.2$  Hz), 7.35 (1H, d,  $J = 7.6$  Hz), 7.13 (1H, d,  $J = 7.2$  Hz), 6.73 (1H, d,  $J = 8.0$  Hz), 6.55 (1H, d,  $J = 9.2$  Hz), 6.433 (1H, s), 6.34 (1H, d,  $J = 8.8$  Hz) 3.33 (4H, q,  $J = 7.2$  Hz), 1.31 (12H, s), 1.14 (6H, t,  $J = 7.2$  Hz).  $^{13}\text{C}$  NMR ( $\text{CDCl}_3/10\% \text{CD}_3\text{OD}$ , 100 MHz):  $\delta$  170.1, 153.2, 152.8, 151.1, 134.9, 129.6, 128.8, 128.8, 127.2, 126.7, 124.9, 124.0, 123.9, 121.8, 84.2, 44.5, 12.4. HR-FABMS: calculated for  $[M^+]$  498.2452, found 498.2441.

**Julolidine Rhodol (11).** Synthesis adopted from literature.<sup>101</sup> 8-Hydroxy-9-*o*-carboxybenzoyljulolidine (3.23 g, 9.56 mmol) and resorcinol (1.05 g, 9.56 mmol) were added to a heavy-walled pressure flask and dissolved in 20 mL of methane sulfonic acid. The reaction contents were heated to 90 °C for 3 h, then cooled to room temperature, and basified with aqueous sodium hydroxide. The mixture was then extracted into ethyl acetate and evaporated under reduced pressure. Purification by column chromatography (4.5:4.5:2 dichloromethane/ethyl acetate/methanol) delivered **11** as a maroon solid (2.5 g, 63% yield).  $^1\text{H}$  NMR ( $\text{CDCl}_3/10\% \text{CD}_3\text{OD}$ , 400 MHz):  $\delta$  8.01 (1H, d,  $J = 7.2$  Hz), 7.46 (2H, quartet,  $J = 8.8$  Hz), 7.02 (1H, d,  $J = 7.2$  Hz), 6.92 (1H, d,  $J = 9.2$  Hz), 6.64 (1H, s), 6.58 (1H, s), 6.49 (1H, d,  $J = 7.6$  Hz), 3.33 (4H, quintet,  $J = 6.0$  Hz), 2.86 (2H, d,  $J = 6.4$  Hz), 2.50–2.58 (2H, m), 1.72–1.99 (4H, m).  $^{13}\text{C}$  NMR ( $\text{CDCl}_3/10\% \text{CD}_3\text{OD}$ , 100 MHz):  $\delta$  174.6, 167.8, 153.9, 148.1, 146.4, 134.0, 126.9, 125.9, 125.8, 125.3, 125.0, 122.9, 118.5, 117.4, 109.7, 108.7, 100.9, 99.0, 46.7, 46.2, 23.4, 16.7, 15.8. HR-FABMS: calculated for  $[M^+]$  412.1549, found 412.1555.

**Julolidine Rhodol Triflate (12).** Compound **11** (500 mg, 1.2 mmol) and *N*-phenyl bis(trifluoromethanesulfonamide) (868 mg, 2.4 mmol) were added to a vial and flushed with nitrogen. The reaction contents were dissolved in 5 mL of DMF, and diisopropylethylamine (805  $\mu\text{L}$ , 4.9 mmol) was added. After 20 min of stirring at room temperature, the product was extracted into ethyl acetate, washed three times with water, and evaporated under reduced pressure. Purification by column chromatography (1:1 hexanes/ethyl acetate) afforded **12** as a light red solid (224 mg, 34%).  $^1\text{H}$  NMR ( $(\text{CD}_3)_2\text{O}$ , 400 MHz):  $\delta$  7.98 (1H, d,  $J = 7.6$  Hz), 7.79 (1H, t,  $J = 7.2$  Hz), 7.73 (1H, t,  $J = 7.6$  Hz), 7.52 (1H, d,  $J = 2.8$  Hz), 7.31 (1H, d,  $J = 7.6$  Hz), 7.15 (1H dd,  $J = 2.4, 8.8$  Hz), 7.00 (1H, d,  $J = 8.8$  Hz), 6.19 (1H, s), 3.20 (2H, t,  $J = 6.0$  Hz), 3.15 (2H, t,  $J = 6.0$  Hz), 2.91 (2H, t,  $J = 6.8$  Hz), 2.41–2.59 (2H, m), 1.92–2.00 (2H, m), 1.76–1.86 (2H, m).  $^{13}\text{C}$  NMR ( $(\text{CD}_3)_2\text{O}/10\% \text{CD}_3\text{OD}$ , 100 MHz):  $\delta$  168.3, 152.5, 152.4, 149.9, 147.3, 144.7, 135.2, 130.3, 130.0, 126.9, 124.6, 124.5, 124.1, 120.7, 118.5, 116.3, 110.4, 106.8, 104.5, 82.6, 49.4, 48.9, 21.4, 20.8, 20.7, 19.9.  $^{19}\text{F}$  NMR ( $(\text{CD}_3)_2\text{O}$ , 376.5 MHz):  $\delta$  -73.284. HR-FABMS: calculated for  $[M^+]$  544.1042, found 544.1036.

**Peroxy Orange 1, PO1 (13).** Compound **12** (100 mg, 0.18 mmol), bis(pinacolato)diboron (47 mg, 0.18 mmol), Pd(dppf) $\text{Cl}_2 \cdot \text{CH}_2\text{Cl}_2$  (45 mg, 0.05 mmol), potassium acetate (55 mg, 0.55 mmol), and 5 mL of toluene were added to a dry pressure tube in an inert

atmosphere glovebox. The pressure tube was then brought out of the box and microwave-heated for 2 h at 110 °C. After cooling the reaction mixture to room temperature, the contents of the pressure flask were washed into a round-bottom flask with dichloromethane and evaporated to dryness. Purification by column chromatography (4.5:4.5:1 dichloromethane/ethyl acetate/methanol) delivered PO1 as light red solid (36 mg, 38%). <sup>1</sup>H NMR (CDCl<sub>3</sub>/10% CD<sub>3</sub>OD, 400 MHz): δ 7.95 (1H, d, *J* = 7.2 Hz), 7.40 (1H, s), 7.58 (1H, t, *J* = 7.2 Hz), 7.54 (1H, t, *J* = 7.2 Hz), 7.33 (1H, d, *J* = 8.0 Hz), 7.11 (1H, d, *J* = 7.6 Hz), 6.69 (1H, d, *J* = 7.6 Hz), 6.10 (1H, s), 3.10 (2H, t, *J* = 5.2 Hz), 3.06 (2H, t, *J* = 5.2 Hz), 2.87 (2H, t, *J* = 6.4 Hz), 2.37–2.54 (2H, m), 1.91–1.99 (2H, m), 1.79 (2H, t, *J* = 5.2 Hz), 1.28 (12H, s). <sup>13</sup>C NMR (CDCl<sub>3</sub>/10% CD<sub>3</sub>OD, 100 MHz): δ 170.1, 153.2, 151.1, 147.8, 144.7, 134.9, 129.5, 128.6, 127.1, 126.8, 124.8, 124.6, 124.0, 123.5, 121.6, 117.8, 107.2, 104.5, 85.1, 84.1, 74.9, 49.7, 49.3, 27.3, 24.8, 21.6, 21.1, 20.9. HR-FABMS: calculated for [M<sup>+</sup>] 522.2456, found 522.2452.

**Spectroscopic Materials and Methods.** Millipore water was used to prepare all aqueous solutions. All spectroscopic measurements were performed in 20 mM HEPES buffer, pH 7. Absorption spectra were recorded on a Varian Cary 50 spectrophotometer (Walnut Creek, CA), and fluorescence spectra were recorded on a Photon Technology International Quanta Master 4 L-format scanning spectrofluorometer (Lawrenceville, NJ) equipped with an LPS-220B 75-W xenon lamp and power supply, A-1010B lamp housing with integrated igniter, switchable 814 photon-counting/analog photomultiplier detection unit, and MD5020 motor driver. Samples for absorption and emission measurements were contained in 1-cm × 1-cm quartz cuvettes (1.5-mL volume, Starna, Atascadero, CA). Fluorescence quantum yields were determined by reference to fluorescein in 0.1 M NaOH ( $\Phi = 0.94$ ) or rhodamine B in water ( $\Phi = 0.31$ ).

**Preparation and Staining of Cell Cultures.** RAW264.7 macrophages were cultured in Dulbecco's Modified Eagle Medium (DMEM) containing high glucose with GlutaMAX (Invitrogen, Carlsbad, CA) and supplemented with 10% Fetal Bovine Serum (FBS, Hyclone). A431 cells were cultured in DMEM plus GlutaMAX supplemented with 10% FBS. Cells were split 1/30 twice a week. Cells were passed and plated on 18-mm glass coverslips coated with poly-L-lysine 2 days before imaging (50 μg/mL, Sigma, St. Louis, MO). A431 cells that were to be used for EGF stimulation experiments were serum-starved in DMEM alone 18 h before imaging. For all experiments, solutions of dyes (from 5 mM stocks in DMSO) were made in DPBS with calcium chloride and magnesium chloride (Sigma). H<sub>2</sub>O<sub>2</sub> (100 mM stock solution in Millipore water), HOCl (100 mM stock solution in Millipore water), phorbol myristate acetate (PMA, 1 mg/mL stock solution in

DMSO), or EGF (100 μg/mL stock in Millipore water) was added by bath application to the cell culture media. The cells were then kept in an incubator (37 °C, 5% CO<sub>2</sub>) during the course of all experiments.

**Fluorescence Imaging Experiments.** Confocal fluorescence imaging studies were performed with a Zeiss LSM510 NLO Axiovert 200 laser scanning microscope and a 40× or 63× Achromplan IR water-immersion objective lens. Excitation of PF2- and PF3-loaded cells at 488 nm was carried out with an Ar laser, and emission was collected using a META detector between 495 and 581 nm. Excitation of PY1-loaded cells at 514 nm was carried out with an Ar laser, and emission was collected using a META detector between 516 and 581 nm. Excitation of PO1-loaded cells at 543 nm was carried out with a HeNe laser, and emission was collected using a META detector between 548 and 613 nm. Excitation of Hoechst 33342 was carried out using a MaiTai two-photon laser at 780-nm pulses (mode-locked Ti:sapphire laser, Tsunami Spectra Physics), and emission was collected between 452 and 537 nm. Excitation of PO1- and APF-loaded cells at 488 and 543 nm was carried out with Ar and HeNe lasers, respectively, and emission was collected using a META detector at 495–538 and 548–602 nm, respectively, using sequential scans. Image analysis was performed in Image J.

**Acknowledgment.** We thank the Packard and Sloan Foundations, the Hellman Faculty Fund (UC Berkeley), Amgen, Astra Zeneca, Novartis, and the National Institute of General Medical Sciences (NIH GM 79465) for funding this work. C.J.C. is an Investigator with the Howard Hughes Medical Institute. B.C.D. thanks the NIH Chemical Biology Graduate Program (T32 GM066698) for support, and C.H. thanks the Department of Chemistry at UC Berkeley for a Summer Undergraduate Research award. We thank Holly Aaron (UCB Molecular Imaging Center) and Ann Fischer (UCB Tissue Culture Facility) for expert technical assistance and helpful discussions.

**Note Added after ASAP Publication.** The formula for the reagent used to treat the parent dye was incorrect in Schemes 2 and 3 in the version of this article published ASAP April 2, 2010. The corrected version was reposted April 7, 2010.

**Supporting Information Available:** Additional imaging data. This material is available free of charge via the Internet at <http://pubs.acs.org>.

JA1014103